Technical University Ilmenau

Faculty of Computer Science and Automation

Group Studies

Water Quality Modeling in Water Distribution System

Submitted by: Timur Gubaev (Matrikelnr.: 63447)
Roman Mysianov (Matrikelnr.: 63450)
Ilia Kuzin (Matrikelnr.: 63482)

Date of submission: March 25, 2022

Study course: Technical Cybernetics and Systems Theory

Supervisor: Prof. Dr.-Ing. habil. Pu Li

Advisor: M.Sc. Hao Cao

Semester: WS2020/2021

Contents

List of Abbreviations

WDN	water distribution network
WDS	water distribution system
THM	trihalomethane
ODE	ordinary differential equation
PDE	partial differential equation
SADHL	squared accumulated directed head losses
nRMSD	normalized root mean squared deviation
anRMSD	average normalized root mean squared deviation

List of Symbols

C_h	Hazen-Williams coefficient of pipe
C_i	concentration of a chemical in the i-th pipe $[\frac{mg}{ft^3}]$
C_L	limiting concentration $[\frac{mg}{ft^3}]$
D	molecular diffusivity $[\frac{ft^2}{t}]$
D	vector of demands
d_i	diameter of the i-th pipe $[ft]$
H_f	vector of head losses
h_i	head loss of i-th pipe $[ft]$
I_k	set of pipeswith inflows into the k-th junction
K_b	bulk flow reaction rate constant
k_f	mass transfer coefficient $[\frac{ft}{t}]$
k_i	head loss per unit flow of i-th pipe $[\frac{s}{ft^2}]$
k_w	pipe wall reaction rate constant $[\frac{ft}{t}]$
L	matrix of cycle-flow associations
L_i	length of the i-th pipe $[ft]$
l_{ij}	association between i-th cycle and j-th flow
N	matrix of node-flow associations
n_{ij}	association between i-th node and j-th flow
Q	vector of flows
q_i	flow in the i-th pipe $[\frac{ft^3}{s}]$
R_i	reaction rate in the i-th pipe $[\frac{mg}{ft^3 t}]$
r_i	radius of the i-th pipe $[ft]$
Re	Reynolds number
Sc	Schmidt number
Sh	Sherwoord number

t	time $[s]$
x	distance $[ft]$

Abstract

The objective of water quality modeling in water distribution systems (WDS) is to predict the spatial and temporal distribution of constituents in a pipe network concerning varying flow conditions. The disinfectant content, usually residual chlorine is one of the most popular parameters certifying the quality of transported water [8] and is modeled using methods investigated in the current paper. These methods allow the prediction of the disinfectant concentration for each spatio-temporal point while EPANET allows predicting an average concentration in time.
The Hardy Cross method and the method of maximization of energy conservation introduced in the current work are used to solve the non-linear system of hydraulics equations. These methods are then compared by their consumption of computational time.
At first, the transport of water in WDS is modeled by the advection equation with the bulk flow and pipe wall reaction terms. This equation is solved using the semi-discrete upwind scheme [11] with different ordinary differential equations (ODE) solvers. The efficiency comparison of these methods is provided as well as their verification by comparing the obtained results with those of EPANET.
The last part of this paper describes modeling the transport of water by the advection-dispersion equation not modeled by EPANET. This equation is numerically solved by the Crank-Nicolson method.

1 Introduction

Water is one of the most precious of our recyclable resources and is used for drinking, washing, agriculture, and industry. It is most important that the water which people drink and use for other purposes meets quality standards. Water quality standards require the minimization of harmful biological formations and disinfection by-products (DBPs) found in the drinking water.
The concept of water as a natural resource, which must be carefully managed, is becoming increasingly important as its appreciation increases. The derivation of the most effective management strategies relies on using mathematical models and simulations. Therefore, reliable and accurate water quality models and efficient mechanisms of their evaluation are needed.
In this paper, the disinfectant concentration as one of the most important indicators of water quality is considered. It is influenced by variations of its demand at different nodes of WDN as well as different chemical reactions and variations of the disinfectant concentration at reservoirs.

1.1 Problem Definition

Because of the long travel time in the network, water loses its quality. Usually, long residence time leads to the microbial formation in the pipe walls and the disinfectant decays with time. In the modern world interest in the study of water quality in distribution systems using mathematical models is increasing rapidly. Early works of Hardy Cross formed a mathematical concept to analyze WDS. Further, these ideas were developed by various researchers including Lewis Rossman. This has lead to the creation of EPANET [16] — a public domain, water distribution system modeling software package. EPANET is still in use by many researchers and companies interested in modeling drinking water quality. However, it does not allow to analyze water quality in each spatial point of a WDN. Moreover, the dispersion phenomena occurring in the transport of drinking water through a WDS has a high impact on water quality analysis [8], but it is not modeled by EPANET.

1.2 Research Objectives

This research is dedicated to disinfectant concentration modeling in a WDN. The flow distribution in the network must be accurately known to model the spatial and temporal distribution of a constituent. Methods for flow calculation and chemical concentration modeling are needed such that the concentration is known in each spatial point of a WDN. The comparison between the introduced methods and EPANET is to be carried out. The modeling of the advection-dispersion transport must be implemented and analyzed.

2 Theoretical Framework

2.1 Definition of Water Quality

The quality of water delivered to the customers depends on its initial chemical and physical composition, the proper choice of purification technology, technical condition of water storage tanks and the WDN as well as hydraulic conditions and exploitation manner of the WDS [12].
The water quality is determined by: oxygen decay, disinfectant decay, the formation of disinfection by-products (trihalomethanes, THMs), change of color, smell and turbidity. The disinfectant content, usually residual chlorine is one of the most popular parameters certifying the quality of transported water. Maintenance of residual chlorine minimal concentration inside the whole WDS protects water against microorganism development and deterioration of its quality parameters.
Chlorine propagation inside the WDS may be studied with the use of mathematical models comprehensively describing the variable hydraulic conditions and reflecting individual factors influencing the disinfectant decay. Modeling of water quality in this case may be understood as the monitoring of water quality parameters increase or decrease.
Chlorine added to water during the process of disinfection reacts with organic and non-organic matter. Thus, the residual chlorine decay in time, regardless of the other factors influencing its decay, is observed. The decrease of chlorine concentration below the minimal level may cause secondary development of microorganisms. Otherwise, excessive chlorine dose added to water during disinfection process may cause formation of dangerous disinfection by-products.

2.2 Mathematical Analysis

2.2.1 Hydraulics

Any WDN can be represented as a finite directed graph with n_c elementary cycles where n_n vertices are associated with junctions and n_l edges are associated with pipes respectively. An example network in EPANET depicted in Fig. 2.1 has 5 elementary cycles. Adjacency matrix of such graph can be used to derive the following matrix that associates cycles and flows:

$$L = \begin{bmatrix} l_{11} & l_{12} & \dots & l_{1n_l} \\ l_{21} & l_{22} & \dots & l_{2n_l} \\ \vdots & \vdots & \ddots & \vdots \\ l_{n_c1} & l_{n_c2} & \dots & l_{n_cn_l} \end{bmatrix}, \quad l_{ij} \in \{-1, 0, 1\} \tag{2.1}$$

where each row of the matrix L relates the i-th cycle and n_l pipe flows. The value of an entry l_{ij} is set to 1 if the j-th flow is clockwise relative to the i-th cycle, to -1 if it

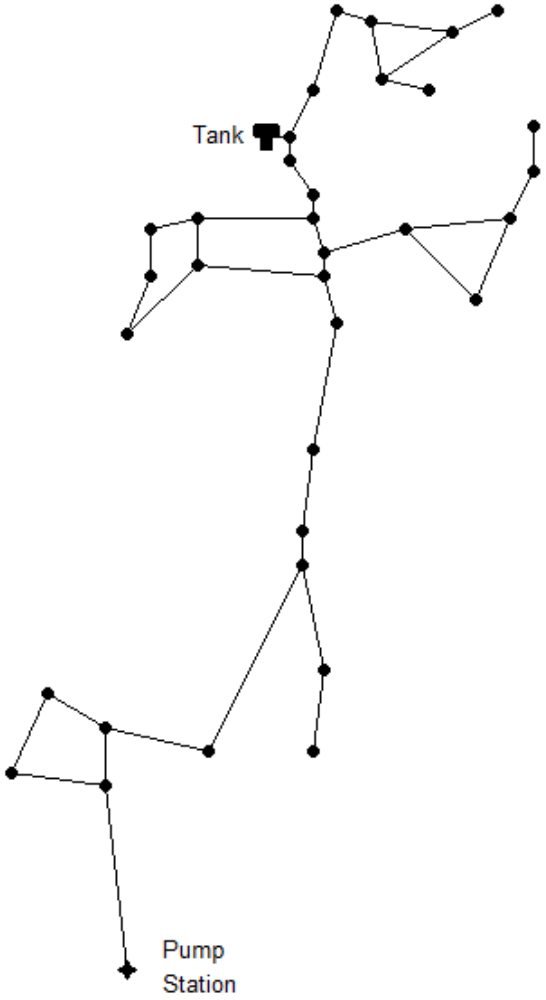

Figure 2.1: Example of a network in EPANET

is counter-clockwise, and to 0 if it is not presented in the cycle. Fig. 2.2 shows a simple network with two cycles. The corresponding value l_{1AC} of the pipe AC is -1 because it has a counter-clockwise direction in the cycle 1. However, the value l_{2AC} for this pipe is 0 since it is not presented in the cycle 2. Another matrix that relates nodes and flows is derived from the adjacency matrix as:

$$N = \begin{bmatrix} n_{11} & n_{12} & \dots & n_{1n_l} \\ n_{21} & n_{22} & \dots & n_{2n_l} \\ \vdots & \vdots & \ddots & \vdots \\ n_{n_n1} & n_{n_n2} & \dots & n_{n_nn_l} \end{bmatrix}, \quad n_{ij} \in \{-1, 0, 1\} \tag{2.2}$$

where each row of the matrix N relates the i-th node and n_l pipe flows. The value of an entry n_{ij} is set to 1 if the j-th flow enters the i-th node, to -1 if the j-th flow leaves the i-th node, and to 0 if the j-th flow is not related to i-th flow.

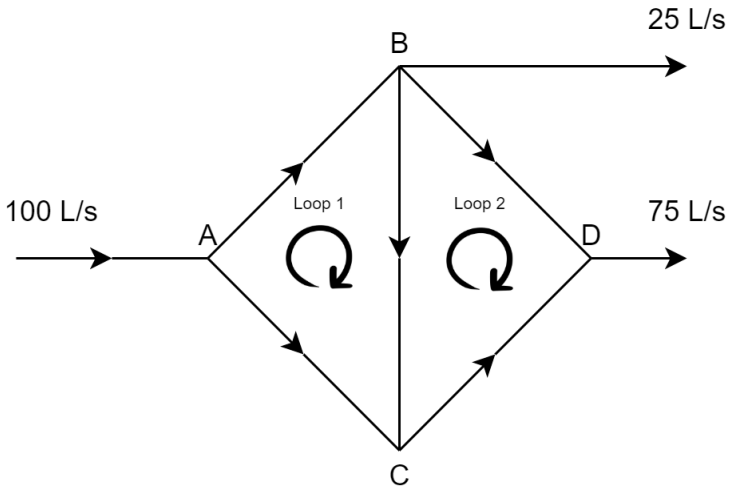

Figure 2.2: Simple network with two cycles

The vector Q of all flows for each pipe in a WDN is defined as:

$$Q = \begin{bmatrix} q_1 & q_2 & \dots & q_{n_l} \end{bmatrix}^T \tag{2.3}$$

Each node of a WDN can have a predefined outflow called demand. The vector D containing demands for all nodes in a WDN is defined as follows (if a node has no demand its corresponding demand value is set to zero):

$$D = \begin{bmatrix} d_1 & d_2 & \dots & d_{n_n} \end{bmatrix}^T \tag{2.4}$$

The general relationship between head loss and flow is:

$$h_i = k_i q_i^n \tag{2.5}$$

where h_i is the head loss of the i-th pipe, k_i is the head loss per unit flow of the i-th pipe, and n is the flow exponent.
There are two most common implementations of the equation 2.5, namely the Darcy-Weisbach and the Hazen-Williams equations. In [14] it is shown that any of these equations can be used to effectively analyze hydraulics in WDNs. The Hazen-Williams equation has been chosen to describe head losses since it has less computational complexity in comparison with the Darcy-Weisbach equation, and it is suitable for the flow of water. The Hazen-Williams equation implies that $n = 1.85$ and k_i is defined as:

$$k_i = L_i \frac{10.67}{C_h^{1.85} d_i} \tag{2.6}$$

where L_i is a length of the i-th pipe, C_h is the Hazen-Williams coefficient, and d_i is a diameter of the i-th pipe. Therefore, the vector H_f of all head losses for each pipe is defined as:

$$H_f = \begin{bmatrix} k_1 q_1^{1.85} & k_2 q_2^{1.85} & \dots & k_{n_l} q_{n_l}^{1.85} \end{bmatrix}^T \tag{2.7}$$

On the one hand, applying the continuity of flow principle the following system of linear equations is obtained:

$$NQ = D \tag{2.8}$$

On the other hand, applying the continuity of potential principle the following system of non-linear equations is obtained:

$$LH_f = \mathbf{0} \tag{2.9}$$

Joint solution of the equations 2.8 and 2.9 produces the vector of known flows for each pipe of a given WDN. Average flow velocities are then found by:

$$u_i = \frac{4q_i}{\pi d_i^2} \tag{2.10}$$

where q_i is a flow in the i-th pipe, and d_i is a diameter of the i-th pipe.

2.2.2 Water Quality with Advective Transport

Before proceeding to the mathematical analysis of water quality modeling, certain assumptions regarding the behavior of hydraulics conditions, water transportation, and chemical reactions are to be made. Flow is assumed to be one-dimensional, hydraulics in WDN is quasi-steady, mixing of flows entering nodes is instantaneous and complete, flow rate is constant throughout a pipe, ideal plug flow with negligible longitudinal dispersion and a single contaminant with one or multiple sources and first order kinetic decay function that occurs at bulk flow and the pipe wall. The same assumptions are used by numerical methods implemented in EPANET [16].
Advective transport without dispersion and constant flow rate within a pipe is described with the following PDE:

$$\frac{\partial C_i}{\partial t} = -u_i \frac{\partial C_i}{\partial x} + R_i(C_i) \tag{2.11}$$

where C_i is a concentration of a chemical in the i-th pipe as a function of time t and distance x, u_i is a flow velocity, and R_i is a reaction rate as a function of the concentration.
Instantaneous and complete mixing of inflows received by a node is described as a simple flow-weighted sum of the concentrations from the in-flowing pipes. The concentration at the beginning of outgoing pipes will be the same and equal to the concentration at a junction (Fig. 2.3). Hence the concentration of the substance leaving the node is as follows:

$$C_i(t, 0) = \frac{\sum_{j \in I_k} q_j C_j(t, L_j)}{\sum_{j \in I_k} q_j} \tag{2.12}$$

where C_i is a concentration in the i-th pipe with outflow from the k-th junction, C_j is a concentration in the j-th pipe with inflow into the k-th junction, I_k is a set of pipes with inflows into the k-th junction, L_j is a length of the j-th pipe, and Q_j is a flow in the j-th pipe. Both the equations 2.11 and 2.12 comprise the DAE modeling

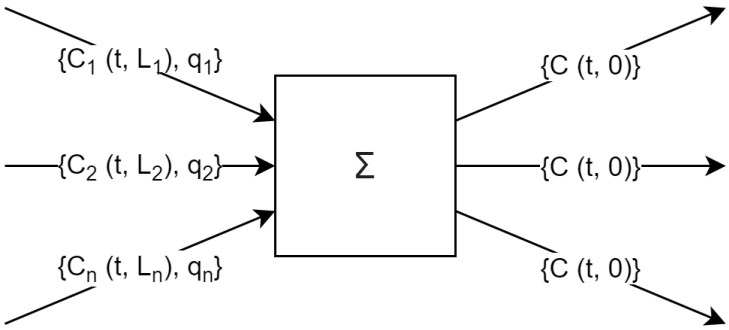

Figure 2.3: Propagation of water through a junction

water quality.
While a substance moves down a pipe it can undergo reaction with constituents in the water column. This phenomenon is called the bulk flow reaction. The rate of the bulk flow reaction can generally be described as a power function of concentration:

$$R_i^{bulk}(C_i) = kC_i^n \tag{2.13}$$

where R_i is a reaction rate in the i-th pipe, k is a reaction constant, and n is the reaction order. When a limiting concentration exists on the ultimate growth or loss of a substance then the rate expression becomes:

$$R_i^{bulk}(C_i) = K_b(C_L - C_i)C_i^{(n-1)} \tag{2.14}$$

where C_L is the limiting concentration, and K_b is the bulk flow reaction coefficient. While flowing through pipes, dissolved substances can be transported to the pipe wall and react with material such as corrosion products or biofilm that are on or close to the wall. The amount of wall area available for reaction and the rate of mass transfer between the bulk fluid and the wall will also influence the overall rate of this reaction. The surface area per unit volume, which for a pipe equals 2 divided by the radius, determines the former factor. The latter factor can be represented by a mass transfer coefficient whose value depends on the molecular diffusivity of the reactive species and on the Reynolds number of the flow [16]. For first-order kinetics, the rate of a pipe wall reaction can be expressed as:

$$R_i^{wall}(C_i) = \frac{2k_w k_f C_i}{r_i(k_w + k_f)} \tag{2.15}$$

where k_w is a wall reaction constant, k_f is a mass transfer coefficient, and r_i is a radius of the i-th pipe. For zero-order kinetics the reaction rate cannot be any higher than the rate of mass transfer:

$$R_i^{wall}(C_i) = \frac{2}{r_i} min\{k_w, k_f C_i\} \tag{2.16}$$

where k_w is a wall reaction constant and has units of mass/area/time. Mass transfer coefficients are usually expressed in terms of a dimensionless Sherwood number:

$$k_f = Sh\frac{D}{d_i} \tag{2.17}$$

where Sh is a Sherwood number, D is a molecular diffusivity of the species being transported along a pipe, and d_i is a diameter of the i-th pipe. In fully developed laminar flow, the average Sherwood number along the length of a pipe can be expressed as:

$$Sh = 3.65 + \frac{0.0668\frac{d_i}{L_i}ReSc}{1 + 0.04[\frac{d_i}{L_i}ReSc]^{\frac{2}{3}}} \tag{2.18}$$

where Re is the Reynolds number, and Sc is the Schmidt number (kinematic viscosity of water divided by the diffusivity of the chemical). For turbulent flow the empirical correlation of Notter and Sleicher can be used:

$$Sh = 0.0149Re^{0.88}Sc^{\frac{1}{3}} \tag{2.19}$$

The flow type is determined upon a value of the Reynolds number and the corresponding formula for the Sherwood number is then used.

2.2.3 Water Quality with Advective-Dispersive Transport

Advection-dispersion phenomena occur in many physical situations including the transfer of heat in fluids, flow through porous media, the spread of contaminants in fluids and in chemical separation processes [13]. The one-dimensional advection-dispersion equation describing the transport of solutes assuming first-order decay kinetics has a following form [5]:

$$\frac{\partial C_i}{\partial t} = -u_i\frac{\partial C}{\partial x} + E\frac{\partial^2 C_i}{\partial x^2} - (K_b + R_w)C_i \tag{2.20}$$

when C_i is a solute concentration in the i-th pipe, E is the dispersion coefficient, K_b is the bulk flow rate constant, and R_w is the overall chlorine wall demand. The overall chlorine wall demand that accounts for radial mass transfer and disinfectant decay at the pipe wall is described as [17]:

$$R_w = \frac{k_w k_f}{r_h(k_w + k_f)} \tag{2.21}$$

where k_w is a wall reaction constant, k_f is a mass transfer coefficient, and r_h is a pipe hydraulic mean radius. To eliminate the need of calculating the pipe hydraulic mean radius, the equation 2.15 can be used instead of the equation 2.21. In the case of the advective-dispersive transport the equations 2.20 and 2.12 comprise the DAE system which is to be solved for obtaining the spatio-temporal distribution of chlorine along pipes in a WDN.

2.3 Generic Algorithm for WDN Simulation

Simulation of a WDN can be described as a sequential process of numerical solution of different models including additional steps that are required to solve these models. The generic algorithm for WDN simulation is described as a sequence of following steps:

1. Load a network structure and parameters
2. Use the adjacency matrix to compute matrices L and N
3. Find flows of a WDN using the selected method for flow calculation
4. Adjust the L matrix for reversed flows
5. Use the adjacency matrix to perform a topological sorting
6. For each node of a WDN in a topological order:
   a) Compute a disinfectant concentration distribution for pipes with inflows to this node using the selected method
   b) Compute a disinfectant concentration in this node

Topological sorting implementation is based on a depth-first search: a node is added to the beginning of the list after considering all of its descendants. The matrix L is computed using Tarjan's strongly connected components algorithm [4]. It runs in linear time and has a worst performance of $O(|V| + |E|)$.

3 Hydraulics Modeling

3.1 Hardy Cross method

The Hardy Cross method is an application of continuity of flow and continuity of potential to iteratively solve for flows in a pipe network [6]. One of the possible implementations starts by calculating flow guess-values satisfying the system of linear equations 2.8. After the guess-values obtained flows are corrected iteratively using the following equation produced by the first-order Taylor expansion of the system of non-linear equations 2.9:

$$\Delta q_i^{(k)} = \frac{\sum_{\substack{j=1 \\ l_{ij}\neq 0}}^{n_l} l_{ij} k_j |q_j|^n}{\sum_{\substack{j=1 \\ l_{ij}\neq 0}}^{n_l} n k_j |q_j|^{n-1}}, \quad i = 1, ..., n_c \tag{3.1}$$

where $q_i^{(k)}$ is a flow correction for the i-th cycle at the k-th iteration. The actual correction of flows happens after the calculation of flow corrections $q_i^{(k)}$ using the equation:

$$q_j^{(k+1)} = q_j^{(k)} - \sum_{\substack{i=1 \\ l_{ij}>0}}^{n_c} \Delta q_i^{(k)} + \sum_{\substack{i=1 \\ l_{ij}<0}}^{n_c} \Delta q_i^{(k)}, \quad j = 1, ..., n_l \tag{3.2}$$

where $q_j^{(k+1)}$ is a flow value for the j-th pipe after the k-th iteration. The first sum of the equation above accumulates and applies corrections from cycles where the flow was directed clockwise. The second sum corresponds to cycles with counter-clockwise direction of the flow.
Given a certain accuracy ϵ the stopping criterion of this iterative scheme is defined as the maximum flow correction being not greater the accuracy:

$$\max_{i=1,...,n_c} \{|\Delta q_i|\} \leq \epsilon \tag{3.3}$$

3.2 Maximization of Energy Conservation

The idea behind the introduced method of maximization of energy conservation is similar to the approach described in [15], where nodal pressures of a WDN are found by reformulating the initial hydraulics equations into an optimization problem. The maximization of the energy conservation is the minimization of squared accumulated directed head losses (SADHL) in each cycle of a WDN. Instead of minimizing individual SADHL it is possible to minimize their sum multiplied by a constant. This produces a constrained optimization since flow continuity is to be satisfied (equation 2.8). The final formulation of the non-linear optimization problem with

linear equality constraints is as follows:

$$\min_{q_1,\ldots,q_{n_l}} \{H(Q) = \frac{1}{2}\sum_{i=1}^{n_c}(\sum_{j=1}^{n_l} l_{ij}k_j q_j^n)^2\} \tag{3.4}$$

$$\text{subject to:} \quad NQ = D \tag{3.5}$$

where $H(Q)$ is a total sum of SADHL. The equation above represents a sparse large-scale non-linear optimization problem. The interior-point method is well-suited for this type of problems allowing million decision variables and adequate computational time [7]. The implementation of this method provided by MATLAB can use analytic gradient and Hessian to make the solution process faster and more robust [1]. The gradient vector of the function $H(Q)$ is represented by the following equation:

$$\nabla_Q H(Q) = \begin{bmatrix} nk_1 q_1^{n-1} \sum_{i=1}^{n_c}(l_{i1} \sum_{j=1}^{n_l} l_{ij}k_j q_j^n) \\ nk_2 q_2^{n-1} \sum_{i=1}^{n_c}(l_{i2} \sum_{j=1}^{n_l} l_{ij}k_j q_j^n) \\ \vdots \\ nk_{n_l} q_{n_l}^{n-1} \sum_{i=1}^{n_c}(l_{in_l} \sum_{j=1}^{n_c} l_{ij}k_j q_j^n) \end{bmatrix}, \tag{3.6}$$

The mixed partial derivatives used in the Hessian matrix of the function $H(Q)$ are as follows:

$$\frac{\partial H(Q)}{\partial q_k \partial q_l} = n^2 k_k k_l (q_k q_l)^{n-1} \sum_{i=1}^{n_c} l_{ik} l_{il}, \quad \forall k, l : k \neq l \tag{3.7}$$

The second order partial derivatives used in the Hessian matrix of the function $H(Q)$ are as follows:

$$\frac{\partial^2 H(Q)}{\partial q_k^2} = n(n-1)k_k q_k^{n-2} \sum_{i=1}^{n_c}(l_{ik} \sum_{j=1}^{n_k} l_{ij}k_j q_j^n) + n^2 k_k^2 q_k^{2n-2} \sum_{i=1}^{n_c} l_{ik}^2 \tag{3.8}$$

The Hessian matrix of the sum of SADHL is calculated by the equations 3.7 and 3.8. The initial guess-flow values are to be provided for the method, however they are allowed to violate the equation 2.8 and therefore can be all set to zero. If changes in the water demands between any two consecutive constant-level time periods are not drastic, the solution for the current time period can be used as the initial guess values for the solution of the next time period to make the numerical simulation faster.

4 Water Quality Modeling

4.1 Semi-Discrete Upwind Scheme

Semi-discrete upwind scheme is obtained by approximating the first-order derivative of the concentration w.r.t. distance using the backward finite difference [11]. The final representation of the resulting ODE system is:

$$\begin{cases} \frac{\partial C_1}{\partial t} &= -u\frac{C_1-C_0}{\Delta x} + R(C_1) \\ \frac{\partial C_2}{\partial t} &= -u\frac{C_2-C_1}{\Delta x} + R(C_2) \\ &\vdots \\ \frac{\partial C_m}{\partial t} &= -u\frac{C_m-C_{m-1}}{\Delta x_m} + R(C_m) \end{cases} \tag{4.1}$$

with initial values for concentrations

$$C_1 = C_2 = \cdots = C_m = 0 \tag{4.2}$$

where m is the number of segments, $C_1, C_2, ..., C_m$ are concentrations of segments, Δx is the predefined segment size, Δx_m is a size of the last segment, and C_0 is the concentration in a junction preceding the modeled pipe. The number of segments m is calculated as follows:

$$m = \lfloor \frac{L}{\Delta x} \rfloor + \lceil \frac{L}{\Delta x} - \lfloor \frac{L}{\Delta x} \rfloor \rceil \tag{4.3}$$

Therefore, the size of the last segment x_m is calculated as:

$$\Delta x_m = L - \Delta x \lfloor \frac{L}{\Delta x} \rfloor \tag{4.4}$$

The ODE system 4.1 with initial values 4.2 is then solved numerically using the family of the Runge-Kutta methods. MATLAB provides variable-step solvers for ODE systems such as ode45 and ode15s [2]. While the ode45 solver is used for nonstiff differential equations, the ode15s solver is used for stiff problems, and providing a Jacobian matrix of the right hand side of the equation 4.1 always improves solver efficiency [3]. Denoting the right hand side of the ODE system as $f(t)_i$ for each concentration C_i as:

$$f_i(t) = -u\frac{C_i - C_{i-1}}{\Delta x} + R(C_i) \tag{4.5}$$

entries of the Jacobian matrix are then calculated as follows:

$$\frac{\partial f_i(t)}{\partial C_j} = \begin{cases} -\frac{u}{\Delta x} + K_b + k_f, & i = j \\ \frac{u}{\Delta x}, & i = j+1 \\ 0, & \text{else} \end{cases} \tag{4.6}$$

4.2 Crank-Nicolson Method

The Crank–Nicolson method is a finite difference method used for numerically solving the heat equation and similar partial differential equations [10]. It is a second-order method in time. It is implicit in time and can be written as an implicit Runge–Kutta method, and it is numerically stable. The stencil of the Crank-Nicolson method is depicted in Fig. 4.1. In the case of advective-dispersive transport (equation 2.20)

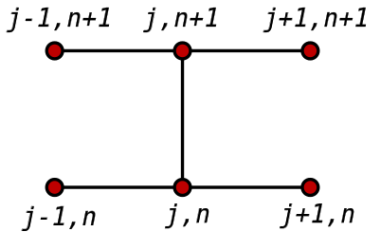

Figure 4.1: Stencil of the Crank-Nicolson method [10]

this method uses the following approximations [13]:

$$\frac{\partial C}{\partial t}\Big|_j^{n+\frac{1}{2}} = \frac{C_j^{n+1} - C_j^n}{\Delta t} \tag{4.7}$$

$$\frac{\partial C}{\partial z}\Big|_j^{n+\frac{1}{2}} = \frac{1}{2}\left[\frac{C_{j+1}^n - C_{j-1}^n}{2\Delta z} + \frac{C_{j+1}^{n+1} - C_{j-1}^{n+1}}{2\Delta z}\right] \tag{4.8}$$

$$\frac{\partial^2 C}{\partial z^2}\Big|_j^{n+\frac{1}{2}} = \frac{1}{2}\left[\frac{C_{j+1}^n - 2C_j^n + C_{j-1}^n}{(\Delta z)^2} + \frac{C_{j+1}^{n+1} - 2C_j^{n+1} + C_{j-1}^{n+1}}{(\Delta z)^2}\right] \tag{4.9}$$

$$C_j^{n+\frac{1}{2}} = \frac{C_j^{n+1} + C_j^n}{2} \tag{4.10}$$

where Δz is a fixed spatial step, and Δt is a fixed time step. Introducing parameters s and c as:

$$s = D\frac{\Delta t}{(\Delta z)^2} \tag{4.11}$$

$$c = u\frac{\Delta t}{\Delta z} \tag{4.12}$$

allows the final equation which approximates the equation 2.20 to be represented in the following form:

$$\begin{aligned} -(c+2s)C_{j-1}^{n+1} + (4+4s+2k\Delta t)C_j^{n+1} - (2s-c)C_{j+1}^{n+1} \\ = (c+2s)C_{j-1}^n + (4-4s-2k\Delta t)C_j^n + (2s-c)C_{j+1}^n \end{aligned} \tag{4.13}$$

where k is the first-order kinetics constant. The resulting equation 4.13 is solved by the Thomas algorithm. The von Neumann method shows that that the equation solved by the Thomas algorithm is stable if:

$$c \leq 2s \tag{4.14}$$

5 Simulation

To perform the simulation the network depicted in Fig. 5.1 is used. It has one reservoir with a constant disinfectant concentration, a pump to create a sufficient pressure, 9 nodes each having a demand and 10 pipes. The Hazen-Williams roughness coefficient is the same for all pipes as well as the bulk flow and pipe wall reaction constants. Tables 5.1 and 5.2 contain parameters of pipes and junctions respectively.

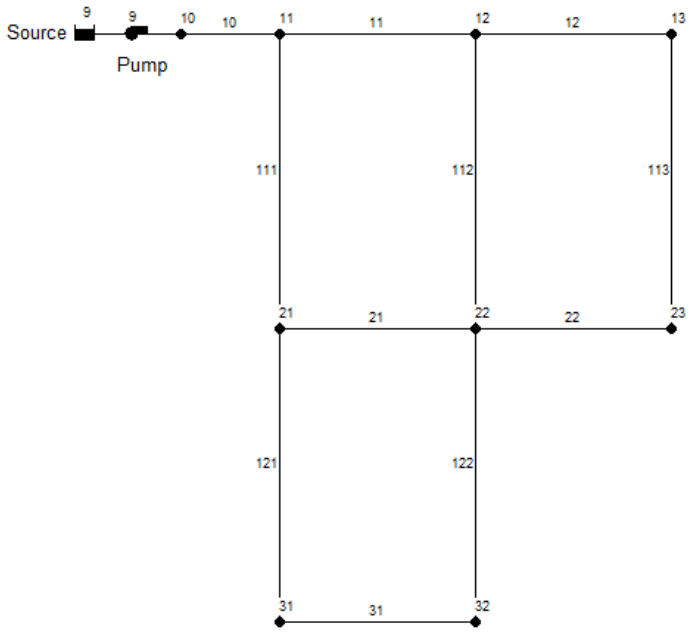

Figure 5.1: Network used for the simulation

Link ID	Length ft	Diameter in	Roughness	Bulk Coeff.	Wall Coeff.
Pipe 10	**10530**	**18**	**100**	**-.5**	**-1**
Pipe 11	**5280**	**14**	**100**	**-.5**	**-1**
Pipe 12	**5280**	**10**	**100**	**-.5**	**-1**
Pipe 21	**5280**	**10**	**100**	**-.5**	**-1**
Pipe 22	**5280**	**12**	**100**	**-.5**	**-1**
Pipe 31	**5280**	**6**	**100**	**-.5**	**-1**
Pipe 111	**5280**	**10**	**100**	**-.5**	**-1**
Pipe 112	**5280**	**12**	**100**	**-.5**	**-1**
Pipe 113	**5280**	**8**	**100**	**-.5**	**-1**
Pipe 121	**5280**	**8**	**100**	**-.5**	**-1**
Pipe 122	**5280**	**6**	**100**	**-.5**	**-1**

Table 5.1: Pipe Network Parameters (Pipes)

The node 22 has a variable demand during 12 hours which consists of 12 constant level demands. The demand pattern of the node 22 is shown in Fig. 5.2.

	Junc 10	Junc 11	Junc 12	Junc 13	Junc 21	Junc 22	Junc 23	Junc 31	Junc 32
Base Demand GPM	0	150	150	100	150	200	150	100	100
Initial Quality mg/L	1	0	0	0	0	0	0	0	0

Table 5.2: Pipe Network Parameters (Junctions)

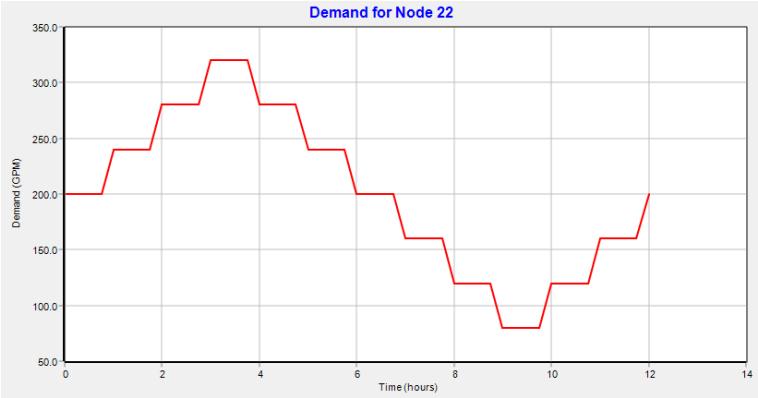

Figure 5.2: Demand pattern for the node 22

5.1 Comparison of Hydraulics Modeling Methods

Two methods of flow calculation have been compared, namely the Hardy Cross method and maximization of energy conservation. There were 100 experiments to calculate flows for a simulation of 12 hours. The measurements of time consumption of each of the methods have been compared using the two-sample t-test with 5% significance level. The test has resulted in rejecting the null hypothesis that mean values of time consumption for each method are the same. The box plot in Fig. 5.3 shows the difference between time consumption of both methods. The experiment

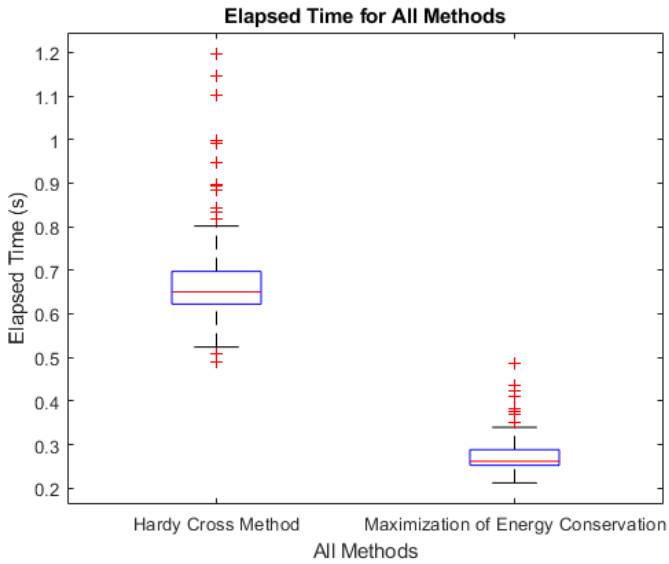

Figure 5.3: Time consumption comparison of the Hardy Cross method and maximization of energy conservation

shows that maximization of energy conservation consumes approximately 2.5 times less computational time than the Hardy Cross method. The maximization of energy conservation is chosen to be the method for flow calculation in further simulations.

5.2 Comparison of ODE Solvers in Semi-Discrete Upwind Scheme

The semi-discrete upwind scheme described in the section 4.1 can have one of two ODE solvers as its part. The most efficient ODE solver in a sense of time consumption is to be chosen based on a statistical comparison as it was done for the flow calculation methods. An experiment consisting of 100 trials with the segment size of 250 feet has been conducted to obtain time consumption measurements for each ODE solver. The two-sample t-test with 5% significance level has shown that there is a statistically significant difference between mean time consumption of two ODE solvers. The box plot in Fig. 5.4 shows the difference in efficiency between two ODE solvers.
The experiment shows that ode15s is approximately 5 times faster than ode45. The ode15s solver is chosen to be used in the semi-discrete upwind scheme in further simulations.

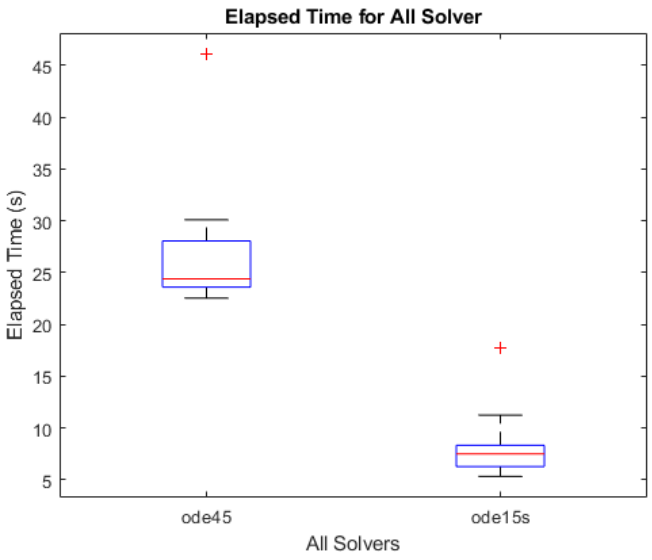

Figure 5.4: Time consumption comparison of ODE solvers

5.3 Comparison of Water Quality Modeling with EPANET

The maximization of energy conservation and the semi-discrete upwind scheme with the ode15s solver are chosen to be compared with EPANET. The previously described network (Fig. 5.1) is used to perform simulations and comparison between EPANET and the chosen methods. The comparison between two approaches is implemented in MATLAB using the EPANET-MATLAB Toolkit [9].
The normalized root mean squared deviation (nRMSD) between concentrations at

the j-th junction in EPANET and MATLAB is used in the comparison analysis and has a following form:

$$nRMSD_j^{junc} = \frac{\sqrt{\frac{1}{n_t}\sum_{t=1}^{n_t}(C_{tj}^{EPANET} - C_{tj}^{MATLAB})^2}}{\frac{1}{n_t}\sum_{t=1}^{n_t} C_{tj}^{MATLAB}} \tag{5.1}$$

where n_t is the number of time points. The nRMSD between the j-th pipe concentrations in EPANET and MATLAB has a different form since EPANET provides only average concentrations for pipes. Therefore, the nRMSD for the j-th pipe is calculated using:

$$nRMSD_j^{pipe} = \frac{\sqrt{\frac{1}{n_t}\sum_{t=1}^{n_t}(C_{tj}^{EPANET} - \frac{1}{m}\sum_{i=0}^{m-1} C(i\Delta x)_{tj}^{MATLAB})^2}}{\frac{1}{n_t}\sum_{t=1}^{n_t}\frac{1}{m}\sum_{i=0}^{m-1} C(i\Delta x)_{tj}^{MATLAB}} \tag{5.2}$$

where m is the number of segments. The formula for the total deviation between EPANET and MATLAB is obtained using equations 5.1 and 5.2 to form an averaged nRMSD:

$$anRMSD = \frac{1}{n_n}\sum_{i=1}^{n_n} nRMSD_i^{junc} + \frac{1}{n_l}\sum_{i=1}^{n_l} nRMSD_i^{pipe} \tag{5.3}$$

The anRMSD between EPANET and MATLAB has been calculated for different segment sizes in the range from $50ft$ to $1000ft$. The linear regression model of the experiment (Fig. 5.5) obtained using the least squares estimation (LSE) shows that the anRMSD linearly decreases with the decrease of the segment size. The time

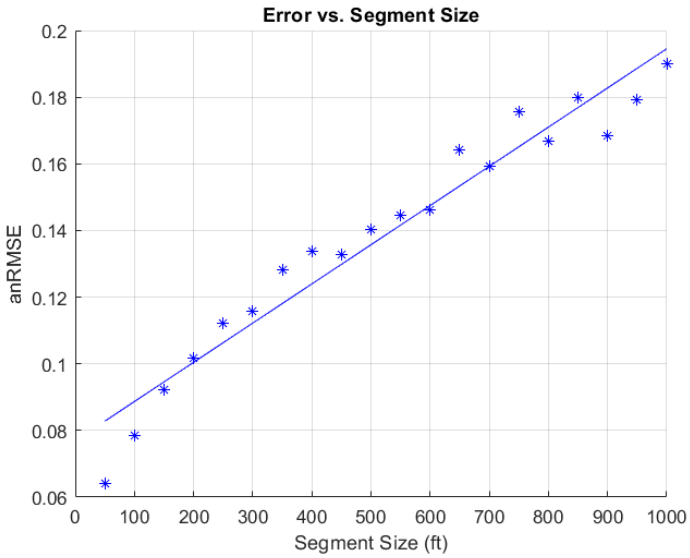

Figure 5.5: The relation between anRMSE and the segment size

consumption of the implemented method grows exponentially with the decrease of the segment size which is shown in Fig. 5.6. The concentration of a disinfectant at the junction 22 is of interest, because it has a variable demand and connects the highest number of pipes among other junctions in the network. The graph comparing the concentration modeling in EPANET and MATLAB is shown in

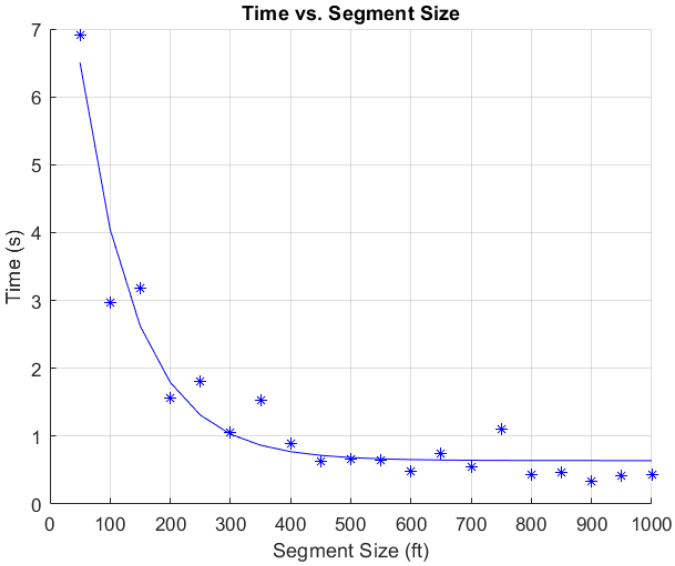

Figure 5.6: The relation between time consumption and the segment size

Fig. 5.7. The curve obtained with MATLAB approach is less stiff than the one obtained with EPANET. This is a result of a numerical dispersion introduced by the semi-discrete upwind scheme. It can be mitigated by further decreasing the segment size. The graphs comparing average concentrations along pipes 111 (Fig.

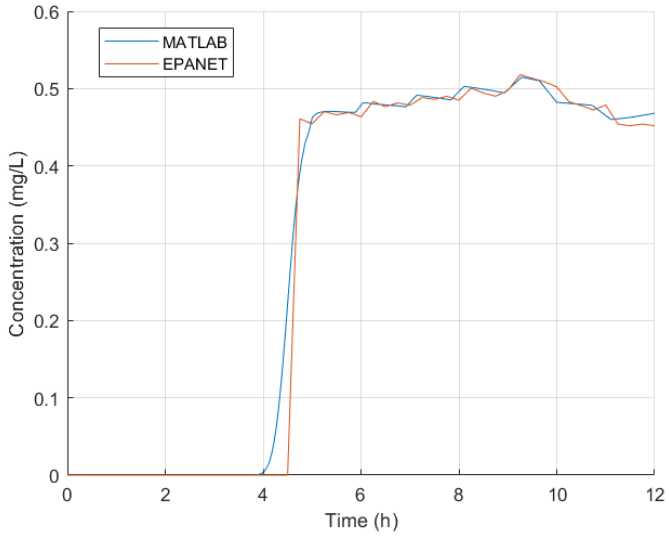

Figure 5.7: Comparison between EPANET and MATLAB in the node 22

5.8) and 122 (Fig. 5.9) show a good agreement between results obtained with EPANET and MATLAB. The concentration transient firstly takes place in the pipe 111 since it is closer to the water source. The disinfectant concentration in the pipe 122 has a peak of approximately $0.4\frac{mg}{L}$ which is explained by the fact that this pipe is affected by many processes in preceding pipes of the network. On of the main objectives of this paper is to create a method which is able to predict spatio-

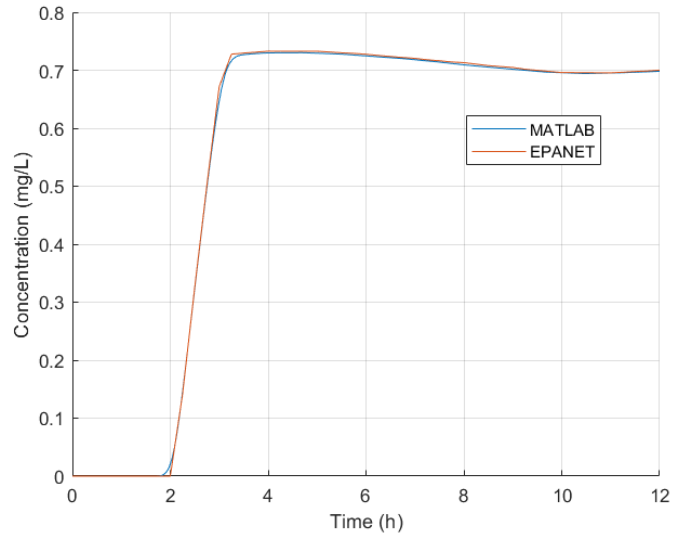

Figure 5.8: Comparison between EPANET and MATLAB at the pipe 111

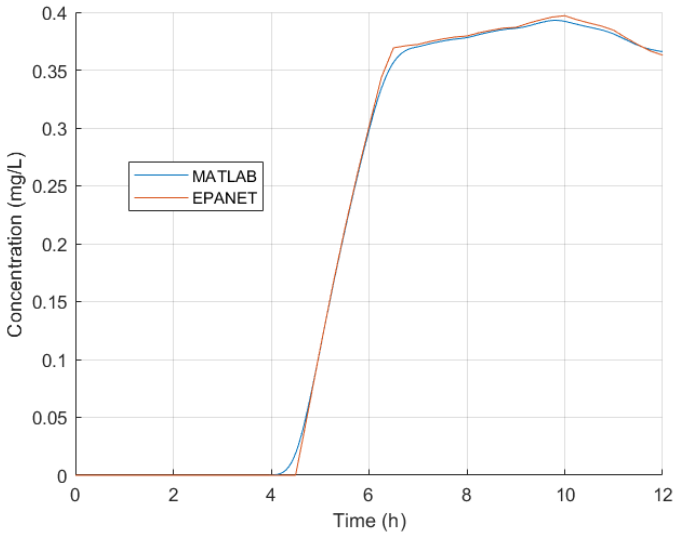

Figure 5.9: Comparison between EPANET and MATLAB at the pipe 122

temporal distribution of a disinfectant concentration in a WDN. The semi-discrite upwind scheme allows to obtain concentration in each point of a WDN for each time instant. Concentrations are calculated for pipe segments of a fixed size and to obtain concentrations in intermediate points a linear interpolation is used. The graphs showing spatio-temporal distribution of a disinfectant concentration for pipes 111 and 122 are shown in Fig. 5.10 and Fig. 5.11. The horizontal axis is a length of a pipe and the vertical axis is a simulation time. In the case of the pipe 111 one can see that its concentration distribution becomes uniform after 12 hours. Since the pipe 122 is more distant from the source than the pipe 111, its concentration does not become uniformly distributed even after 12 hours.

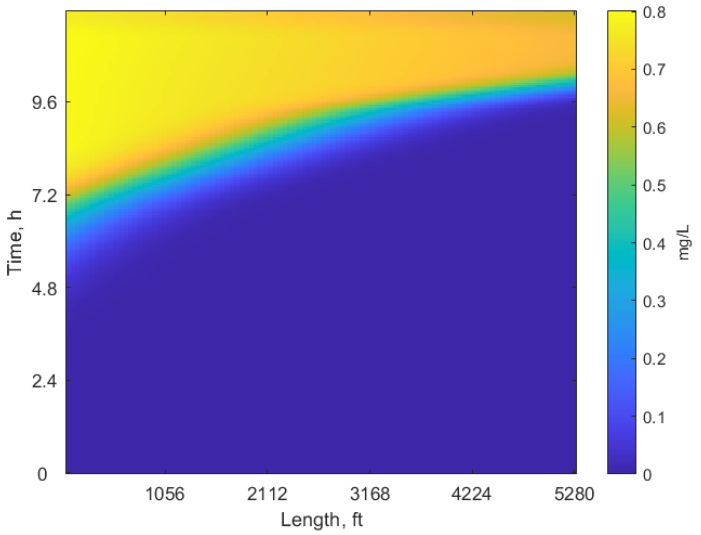

Figure 5.10: Spatio-temporal distribution of a concentration at the pipe 111

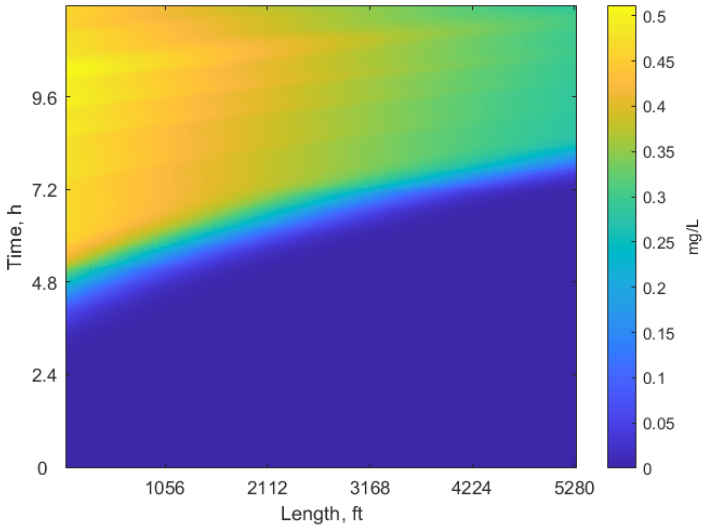

Figure 5.11: Spatio-temporal distribution of a concentration at the pipe 122

5.4 Simulation with Dispersion

To show effects of dispersion, a comparison between a disinfectant concentration in the pipe 21 has been conducted where instead of solving the advective transport, the advective-dispersive transport was simulated. Fig. 5.12 shows how dispersion of $2.5\frac{ft^2}{s}$ affects the time evolution of an average disinfectant concentration in the pipe 21. The maximum concentration has dropped, but traces of the disinfectant appear earlier in time, which is consistent with the dispersion phenomena. The spatio-temporal distribution of the disinfectant concentration under the influence of dispersion is presented in Fig. 5.13.

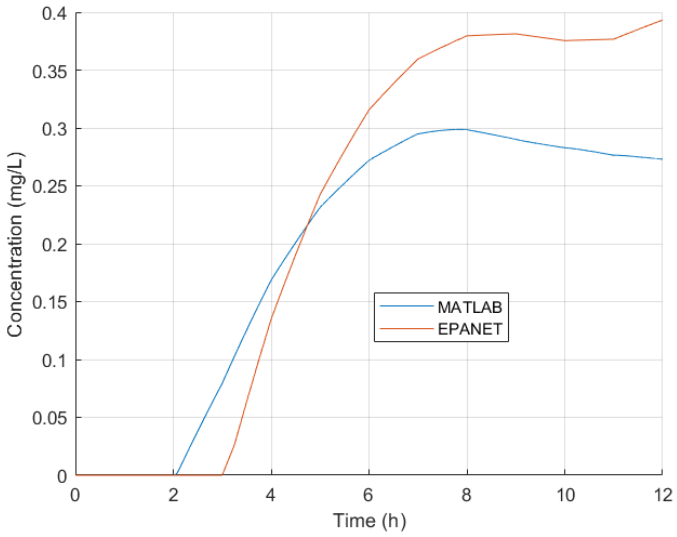

Figure 5.12: Comparison between EPANET and MATLAB approach with dispersion

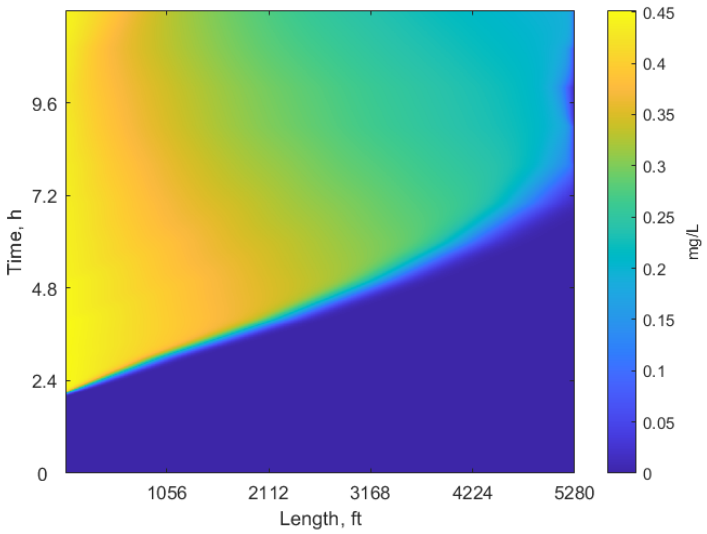

Figure 5.13: Spatio-temporal distribution of a disinfectant under dispersion

6 Conclusion and Future Research Possibilities

It has been shown, that maximization of energy conservation is more effective than the Hardy Cross method. Moreover, the semi-discrete upwind scheme is proved to be the most effective with embedding the ode15s solver. These two methods have been used to obtain the results on the provided network and to compare them with the results of EPANET. The comparison has shown, that the results received from the MATLAB implementation of the above methods are similar to the results of EPANET. However, these methods provide an opportunity to predict a disinfectant concentration for any point of a WDN rather than an average concentration over a whole pipe as it is implemented in EPANET. The Crank-Nicolson method has been implemented to simulate the advective-dispersive transport model. The comparison between EPANET's non-dispersive model and the implemented Crank-Nicolson method has shown the effects of dispersion on the spatio-temporal distribution of a disinfectant concentration.
Future research aims to investigate more efficient methods of flow calculation. The methods for advective and advective-dispersive transport simulation can be improved in such a way that they are more stable and take less computational time to simulate the model. The interaction between different constituents in water could play a significant role in a more accurate prediction of their spatio-temporal distribution. Another important aspect of water quality modeling to be considered in a future research is water quality management which allow to control water quality in a WDN using pressure reducing valves and a real-time control.

Bibliography

[1] *Interior-Point Algorithm with Analytic Hessian.* https://www.mathworks.com/help/optim/ug/fmincon-interior-point-algorithm-with-analytic-hessian.html

[2] *Solve nonstiff differential equations — medium order method.* https://www.mathworks.com/help/matlab/ref/ode45.html

[3] *Solve stiff differential equations and DAEs — variable order method.* https://www.mathworks.com/help/matlab/ref/ode15s.html

[4] *Tarjan's strongly connected component algorithm.* https://www.mathworks.com/matlabcentral/fileexchange/50707-tarjan-e

[5] Abokifa, Ahmed A. ; Maheswari, Abhilasha ; Gudi, Ravindra D. ; Biswas, Pratim: Influence of Dead-End Sections of Drinking Water Distribution Networks on Optimization of Booster Chlorination Systems. In: *Central South University* (2020)

[6] Brkic, Dejan: Short Overview of Early Developments of the Hardy Cross Type Methods for Computation of Flow Distribution in Pipe Networks. In: *Applied Sciences* (2019)

[7] Byrd, Richard ; Hribar, Mary ; Nocedal, Jorge: An Interior Point Algorithm for Large-Scale Nonlinear Programming. In: *SIAM Journal on Optimization* (2009)

[8] Chaudhry, Hanif ; Islam, Rashidul: *Water Quality Modeling in Pipe Networks.* Kluwer Academic Publishers, 1995

[9] Elaides, Demetrios G. ; Kyriakou, Marious ; Vrachmis, Stelios ; Polycarpou, Marios M.: *EPANET-MATLAB Toolkit: An Open-Source Software for Interfacing EPANET with MATLAB.* 2016

[10] Genuchten, M.Th.Van ; Alves, W.J.: Analytical solution of the one-dimentionconvective-dispersive solute transport equation. In: *U.S. Dep. Agric.,Tech.Bull.* (1982)

[11] Molenkamp, Charles: Accuracy of Finite-Difference Methods Applied to the Advection Equation. In: *Journal of Applied Meteorology and Climatology* (1998)

[12] Musz, Anna ; Kowalska, Beata ; Widomski, Marcin: Some Issues Concerning the Problems of Water Quality Modeling in Distribution Systems. In: *Ecological Chemistry and Engineering* (2009)

[13] Najafi, Saberi ; Hajenezhad, Haniye: Solving one-dimensional advection-dispersion with reaction using some finite-difference methods. In: *Applied Mathematical Sciences* (2008)

[14] Nwajuaku, I.I. ; Wakawa, Y.M. ; Adibeli, O.J.: Analysis of Head-loss Equations under EPANET and Hardy Cross Method. In: *Saudi Journal of Engineering and Technology* (2017)

[15] Pecci, Filippo ; Abraham, Edo ; Stoianov, Ivan: Penalty and relaxation methods for the optimal placement and operation of control valves in water supply networks. In: *Springer* (2016)

[16] Rossman, A. L.: *EPANET 2 Users Manual*. United States Environmental Protection Agency, 2000

[17] Rossman, Lewis ; Clark, R.M.: Modeling chlorine residuals in drinking water distribution systems. In: *Journal of Environmental Engineering* (1994)

List of Figures

Statutory Declaration

I declare that I have authored this thesis independently, that I have not used other than the declared resources, and that I have explicitly marked all material which has been quoted either literally or by content from the used sources.

Ilmenau, March 25, 2022 Timur Gubaev

Ilmenau, March 25, 2022 Roman Mysianov

Ilmenau, March 25, 2022 Ilia Kuzin